2015

Oxygen diffusivity in alumina scales grown on Al-MAX phases

James L. Smialek
NASA Glenn Research Center, james.l.smialek@nasa.gov

Corrosion Science 91 (2015) 281–286

Contents lists available at ScienceDirect

Corrosion Science

journal homepage: www.elsevier.com/locate/corsci

Oxygen diffusivity in alumina scales grown on Al-MAX phases

James L. Smialek

National Aeronautics and Space Administration, Glenn Research Center, Cleveland, OH 44135, United States

ARTICLE INFO

Article history:
Received 17 September 2014
Accepted 17 November 2014
Available online 25 November 2014

Keywords:
A. Ceramic
B. Thermal cycling
C. Oxidation
C. High temperature corrosion

ABSTRACT

Ti_3AlC_2, Ti_2AlC, and Cr_2AlC are oxidation resistant MAX phase compounds distinguished by the formation of protective Al_2O_3 scales with well controlled kinetics. A modified Wagner treatment was used to calculate interfacial grain boundary diffusivity from scale growth rates and corresponding interfacial grain size, based on the pressure dependence of oxygen vacancies and diffusivity. MAX phase data from the literature yielded grain boundary diffusivity nearly coincident with that for Zr-doped FeCrAl (and many other FeCrAl alloys), suggesting similar oxidation mechanisms. The consolidated body of diffusivity data was consistent with an activation energy of 375 ± 25 kJ/mol.

Published by Elsevier Ltd.

1. Introduction

MAX phase compounds represent a unique class of ceramic materials with exceptional strain and damage tolerance, thermal shock resistance, and machinability [1]. Here 'M' refers to early period transition metals, 'A' to Group A metals and semimetals, and 'X' to carbon and nitrogen. While over 60 compounds have been reported, a much smaller subset claims optimum oxidation resistance at temperatures greater than 1000 °C. These include Ti_3AlC_2, Ti_2AlC, and Cr_2AlC, which are the primary compounds reported to develop protective alumina scales [2–4]. These properties and attractive thermal expansion matches with alumina, YSZ, (yttria stabilized zirconia) or Ni alloys make alumina-forming MAX phase compounds an interesting option for hybrid high temperature systems with possible implications for turbine components [5].

As with oxidation resistant metals, alumina scale growth on MAX phases has been identified to be controlled by grain boundary diffusion, primarily oxygen. Here scale grain "growth" or enlargement can reduce the number of fast through-paths and directly slow the rate of scale thickening [6–8]. Grain boundary diffusion is typically assumed to be rapid transport along a narrow interfacial region (width δ) of two adjacent gains. The precise analyses of scale microstructure in Refs. [6–8] proved that grain enlargement leads to sub-parabolic (cubic or quartic) oxidation kinetics, analogous to prior treatments of alumina scales on FeCrAl(X)-type alloys. Furthermore, estimates of oxygen grain boundary diffusion were calculated from growth kinetics, grain size, and modified Wagner models of scale growth that will be elaborated on later. Here excellent agreement was obtained between Ti_3AlC_2 [6] and FeCrAl–Y_2O_3 [9], suggesting a commonality of the basic, rate-controlling, transport mechanism.

In that regard, another solution to the Wagner integral has been recently proposed [10]. It again relates oxidation rate to ionic diffusivity, but integrated across the oxygen chemical potential gradient in the scale. It thus takes into account the variation of grain boundary diffusivity across the scale according to $p_{O_2}^{-1/6}$. This dependence had been developed from elegant permeability studies of bulk polycrystalline alumina that produced the following Arrhenius relation for diffusivity [11]:

$$\delta D_{gb,O} = 2.207 \times 10^{-9} \exp\left(\frac{-Q}{RT}\right) p_{O_2}^{-1/6} \quad (1)$$

where Q is equal to 467 kJ/mol (with p_{O_2} in Pa and $D_{gb,O}$ in m^3/s). Here grain boundary diffusion had been characterized as a function of temperature and the pressure differential across a thin polycrystalline alumina wafer. Oxygen diffusivity was found to vary as $p_{O_2}^{-1/6}$, in accord with a doubly charged oxygen vacancy defect, and aluminum diffusivity as $p_{O_2}^{+3/16}$, in accord with a triply charged aluminum vacancy defect [11]. That study has thus provided a long-standing missing link in the complete solution to the classic Wagner integral. A concise working solution was developed previously [10], as briefly outlined below.

Although grain enlargement results in sub-parabolic overall scale growth rates, the Wagner treatment can still be applied to an instantaneous or differential parabolic rate constant, $k_{p,i}$. The conventional form of the Wagner equation, assuming primary control by oxygen diffusivity, is given by Eq. (2a) [10]:

$$k_p = \frac{x^2}{t} = \int_{p_{O_2,int.}}^{p_{O_2,gas}} D_{eff,O}\, d\ln p_{O_2} \quad (2a)$$

E-mail address: james.l.smialek@nasa.gov

http://dx.doi.org/10.1016/j.corsci.2014.11.030
0010-938X/Published by Elsevier Ltd.

It is then coupled with standard relations for the effective diffusivity, $D_{eff} \approx 2\delta D_{gb}/G$, when dominated by grain boundary diffusivity for α-Al_2O_3 [10]. Since the instantaneous $k_{p,i}$ is given by $2x\,dx/dt$, the following Wagner integral is obtained:

$$k_{p,i} = 2x\frac{dx}{dt} = \int_{p_{O_2,int.}}^{p_{O_2,gas}} \frac{2\delta D_{gb,O}}{G_i}\, d\ln p_{O_2} \tag{2b}$$

Here δ is the grain boundary width (~1 nm), $D_{gb,O}$ is oxygen diffusivity (m^2/s) within the grain boundary, x is scale thickness (m), and G_i is the instantaneous grain diameter (m). Integration is performed over the p_{O_2} gradient across the scale, where $p_{O_2,int}$ refers to the equilibrium oxygen pressure at the scale-metal interface, and $p_{O_2,gas}$ refers to the external oxygen partial pressure. By substitution of Eq. (1) and recognizing that $1/p_{O_2,int} \ggg 1/p_{O_2,gas}$, an accurate simplification of Eq. (2b) was obtained [10]. It provides $\delta D_{gb,O}$ in terms of the instantaneous parabolic rate constant ($k_{p,i}$) and the corresponding grain diameter at that time (G_i):

$$\Pi_i = k_{p,i}G_i \approx 12\delta D_{gb,O,int.} \tag{3}$$

(This approach essentially parallels that set forth by Pint et al., albeit with minor alterations) [12,13]. By applying this to a large data set (for x and G versus T, t) in the oxidation of a FeCrAl(Zr) heater alloy (Hoskins 875), it was then found that [10]:

$$\delta D_{gb,O,int.} = 1.8 \times 10^{-10} \exp\left(\frac{-Q}{RT}\right) \tag{4}$$

where Q was determined to be 375 kJ/mol. The diffusivities defined by Eq. (4) are about an order of magnitude lower than those predicted by the permeability Eq. (1) measured for bulk undoped alumina, but applied to the low p_{O_2} interface. This oxygen scale diffusivity is presumed to be the primary rate determining mechanism and is well above (by 4 orders of magnitude) the diffusivity measured in typical atmospheric studies of bulk alumina [11].

This was a reasonable baseline for other FeCrAl alloys as well, to be shown in detail later as representative of a well-characterized alumina-forming system. The purpose of the present work is to assess diffusional control of alumina scale growth on MAX phase compounds using the same treatment. The analysis is enabled by the concept of a constant oxidation product, Π, Eq. (3), which couples instantaneous growth rates with instantaneous grain size of the scales. This solution of the modified Wagner equation, using the $p_{O_2}^{-1/6}$ dependence of diffusion, leads to more appropriate (high) values of $\delta D_{gb,O}$ that apply to the low p_{O_2} growth interface. Data sets, where the time dependence of both scale thickness and interfacial grain diameter were available, produced the most robust results. Some estimates of $\delta D_{gb,O}$ were also included where only average growth rate and grain diameters were reported.

In short, we reduce the published oxidation kinetics of alumina scales formed on Ti_3AlC_2, Ti_2AlC, and Cr_2AlC alumina-forming MAX phases to a single, unifying parameter, oxygen grain boundary diffusivity. This is then critically compared to previously analyzed data for alumina scales formed on FeCrAl(X) alloys. Both data sets are found to be in general agreement with a common activation energy. This reinforces the concept of a similar overall transport mechanism for alumina scales formed on a variety of substrate compositions.

2. Results and discussion

Diffusivity analyses of Ti_3AlC_2 oxidation had been performed over a range of temperatures [6]. Both instantaneous k_p and grain size were measured for 0–20 h oxidation at 1000°, 1150°, and 1250 °C. Since grain size was only given for 1250 °C, the initial calculation of $\delta D_{gb,O,int.}$ from Eq. (4) was limited to that temperature, and shown by the filled 'X' symbol for Ti_3AlC_2 in Fig. 1. The results are seen to be quite close to our fitted line for FeCrAl(Zr). More commonly, $\delta D^{\times}_{gb,O,int.}$. had been assumed to be constant (×superscript) across alumina scales [6,9,14], giving upon integration of Eq. (2b):

$$k_p = \frac{2\delta D^{\times}_{gb,O}}{G}\Delta\ln p_{O_2} \tag{5}$$

This solution of Eq. (2b) then leads to diffusivity values that are 1/6 $\Delta\ln[p_{O_2}]$ those calculated from Eq. (3), [10]. This adjustment can be calculated from the equilibrium oxygen pressure, $p_{O_2,eq}$, as derived from thermodynamics (using the equilibrium reaction constant K_{eq} for the oxidation of aluminum and the activity of aluminum in FeCrAl at the interface). It had been determined for 1000° to 1400 °C [10] from computational thermodynamic codes [15,16] and approximated (in Pa) by this regression fit [10]:

$$p_{O_2,eq} \approx 6.117 \times 10^{15} \exp\left(\frac{-Q}{RT}\right) \tag{6}$$

where Q was determined to be 1012 kJ/mol. Thus the $\delta D^{\times}_{gb,O}$ values reported in Ref. [6], multiplied by 1/6 $\Delta\ln[p_{O_2}]$ (a factor ranging from 11.5 at 1000 °C to 7.8 at 1400 °C), yielded the open 'X' symbols (for Ti_3AlC_2#) in Fig. 1. Good agreement is shown with the prior calculation from Eq. (3) at 1250 °C as well as with the FeCrAl(Zr) baseline. (Note that this treatment for Ti_3AlC_2 assumes a similar and small role of Al activity in the calculation of $p_{O_2,eq}$ from K_{eq} for Ti_3AlC_2 and FeCrAl. [6]).

Next, data for Ti_2AlC is considered. The interfacial grain size and continuous weight gain were obtained at 1200 °C for 80 h. From the power law, where n_i is the instantaneous exponent (~4), the following applies [8]:

$$x^{n_i} = kt \tag{7}$$

Differentiating to obtain dx/dt, and substitution into Eq. (2), it can be shown that:

$$k_{p,i} = \frac{2x_i^2}{n_i t_i} \tag{8}$$

By combining Eqs. (3) and (8), this allows $\delta D_{gb,O,int.}$ to be determined from x_i and n_i versus t given in [8]. The result is shown in Fig. 1 as the upper 'plus' +symbol. Again there is good agreement with the fitted FeCrAl(Zr) line.

Oxidation kinetics and interfacial scale grain size were also measured for Ti_2AlC at 1200 °C for up to 2800 h [7]. Relations for sub-parabolic scale kinetics:

$$x = 1.2(t/t_0)^{0.36} \tag{9}$$

and grain enlargement kinetics:

$$G = 0.295t^{0.31} \tag{10}$$

were reported, where x and G are in (μm) and t in (h). Eq. (9) was used to obtain dx/dt and derive $k_{p,i}$ according to its definition in Eq. (2b). By then combining with Eqs. (10) and (3), $\delta D_{gb,O,int.}$ is given by:

$$\delta D_{gb,O,int.} = 0.254t^{0.03} \tag{11}$$

This indicates a very slight time dependence, with $\delta D_{gb,O,int.}$ ranging from 7 to 9×10^{-24} m^3/s from $t = 1$ to 2800 h. The mid-value of 8.1×10^{-24} m^3/s corresponding to ~100 h is plotted in Fig. 1. Again the diffusion product is seen to agree quite well with the FeCrAl(Zr) baseline. TiO_2 is often observed to some degree in Ti–Al–C MAX phase oxidation and accounts for an initial offset compared to FeCrAl(Zr) [2,3,6–8].

Finally, the oxidation of Cr_2AlC is addressed. Here, data having kinetics with corresponding scale microstructure is sparse. An average parabolic rate constant was reported as 7.5×10^{-11} kg^2/m^4 s at

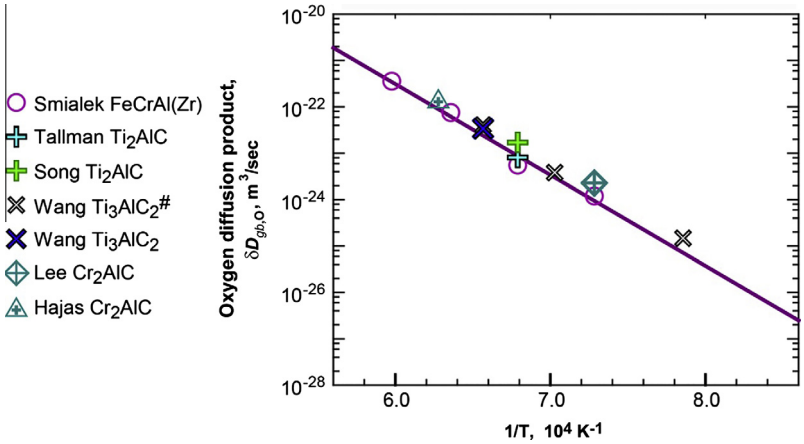

Fig. 1. Arrhenius plot of oxygen grain boundary diffusivity estimated for alumina scales grown on Ti_3AlC_2, Ti_2AlC, and Cr_2AlC MAX phase compounds. Results agree with alloy Hoskins 875 oxidation behavior, i.e., Smialek FeCrAl(Zr), within experimental variability.

1100 °C, 50 h [17]. The same authors had previously presented an interfacial microstructure after 480 h oxidation at 1100 °C [4]. The scale grain size was measured from imprints in the adjacent Cr_7C_3 sublayer as 1.28 ± 0.47 μm. This allows estimates of Π and $\delta D_{gb,O,int.}$, namely 0.10 $(\mu m)^3/h$ and 2.28×10^{-24} m^3/s, respectively. The latter, shown as the crossed diamond in Fig. 1, is seen to be slightly above the fitted line for FeCrAl(Zr) and within a scatter band typical of other MAX phase results.

Another study examined scales formed on sputter coatings of Cr_2AlC during oxidation at 1230–1410 °C for various times [18]. TGA (thermo-gravimetric analyses) revealed near-parabolic kinetics, and grain structure was revealed by means of FIB-XTEM (focused ion beam, cross sectional transmission electron microscopy). Here larger grains are seen to be at the gas-scale interface (scales formed at 1320 °C for up to 5 h), at odds with most studies of alumina scales. Nevertheless the rates are reported to be near those obtained for NiAl and bulk Cr_2AlC. A summary of estimated of grain size, Π, and $\delta D_{gb,O,int.}$ is presented in Table 1. Using the longest time and thickest scale as most representative of the average k_p, the obtained diffusion product (plussed triangle) is seen to agree with the previous data, Fig. 1. However, this value is approximate because an average k_p was used.

Other FeCrAl(X) data. Published Fe20Cr5Al(X) (nominal wt.%) oxidation data is often quoted in comparisons of scale grain boundary diffusivity and was summarized in Ref. [10]. These are presented in Fig. 2 to provide a more global perspective, now all obtained by using Eq. (3) in the same framework as above. Some elaboration of this data is offered below.

A comprehensive study of FeCrAlY oxidation at 1200 °C was presented with detailed microstructural characterizations in [19]. The precise determination of scale grain size as a function of thickness, coupled with an exact polynomial fit of thickness versus oxidation time, allowed the determination of the unique value for $\Pi = 0.455$ $\mu m^3/h$, equivalent to $\delta D_{gb,O,int.} = 1.05 \times 10^{-23}$ [10]. Because of many overlapping points at 1200 °C, the plot is expanded by alloy group in Fig. 3 for clarity. This FeCrAlY datum is quite close to the fitted (dashed) line from the FeCrAl(Zr) Arrhenius plot. Grain diameters were not available for the same FeCrAlY alloy oxidized in another study using Ar–20% O_2 in [14]. However the diffusion integral presented there assumed constant $\delta D^{\times}_{gb,O}$ across the scale thickness, producing a small decrease in the value of $\delta D_{gb,O}$. As with the Ti_3AlC_2 data, these values were multiplied by the $1/6\ \Delta\ln[p_{O_2}]$ correction factor to yield the upper crossed square symbol. The lower symbol corresponds to a similarly corrected value that accounted for grain size variability across the scale thickness [14]. Finally, data for $G = 0.5$ μm scales grown on FeCrAl and FeCrAlY after 100 h at 1200 °C from Pint are shown as the upper and lower triangles, respectively [12,13]. They indicate a reduced diffusivity of ~3× due to Y-doping. Values for the latter FeCrAlY alloys are close and ~2× below the fitted FeCrAl(Zr) line.

Data for the Hoskins 875 FeCrAl(Zr) alloy (Smialek, large circles) were used to define the Arrhenius line in Figs. 1 and 2. However, the 1200 °C value is below the fitted line (Fig. 3) for unknown reasons [10]. This applies to measurements made on numerous separate samples oxidized over a 10, 20, 50, 100, and 200 h time period. By comparison, $\delta D_{gb,O,int.}$ calculated from a single 48 h grain size and fitted k_p for an Imphy FeCrAl(Zr) alloy, similarly doped with 0.2 wt.% Zr, follows the same temperature dependence in Fig. 2, as does their Y-implanted FeCrAl(Zr), but with more scatter [20].

Next we consider a number of studies of the Y_2O_3 oxide-dispersed MA 956 alloy. In one of the earliest modified Wagner treatments of alumina scales, parabolic kinetics were found from 900 to 1200 °C in 25–100 h tests) [21]. While some scatter existed, they described the average behavior (k_p in m^2/s) by one Arrhenius relation:

$$k_p = 1.2 \times 10^{-2} \exp(-Q/RT) \quad (12)$$

where Q was found to be 388 kJ/mol.

A slowly changing, temperature independent interfacial grain size of 0.5 μm was reported, with little elaboration. This allows $\delta D_{gb,O,\ int.}$ to be roughly approximated according to Eq. (3), shown as the crossed circles, quite near the FeCrAl(Zr) baseline in Figs. 2 and 3. In a later study, grain boundary diffusivity was calculated for MA 956 over the same temperature range assuming a constant $\delta D^{\times}_{gb,O}$ across the scale [9]. Grain size was again reported to be relatively temperature independent, but ranged from 0.2 to 1 μm across the thickness, again with insufficient detail to use Eq. (3). The reported $\delta D^{\times}_{gb,O}$ values were therefore multiplied by $1/6\ \Delta\ln[p_{O_2}]$, as discussed for Ti_3AlC_2 and FeCrAlY. Shown as the red stars in Figs. 2 and 3, reasonably good agreement with the FeCrAl(Zr) baseline is observed, except perhaps at 900 °C. The 48 h MA 956 data from [20] (small red circles) yields perhaps the most divergence from the Arrhenius baseline, with no apparent explanation.

Table 1
1320 °C Oxidation product (Π) and scale diffusion product ($\delta D_{gb,O}$) calculated for Cr_2AlC sputtered film. From XTEM grain size and TGA $k_p = 3.16 \times 10^{-9}$ kg^2/m^4 s [18].

Time (h)	G (fine) (μm)	G (coarse) (μm)	Π $((\mu m)^3/h)$	δD_{gb} (m^3/s)
0.065	N.A.	0.13	0.42	9.77×10^{-24}
0.65	0.56	0.71	2.3	5.33×10^{-23}
4.7	0.96	1.71	5.6	1.29×10^{-22}

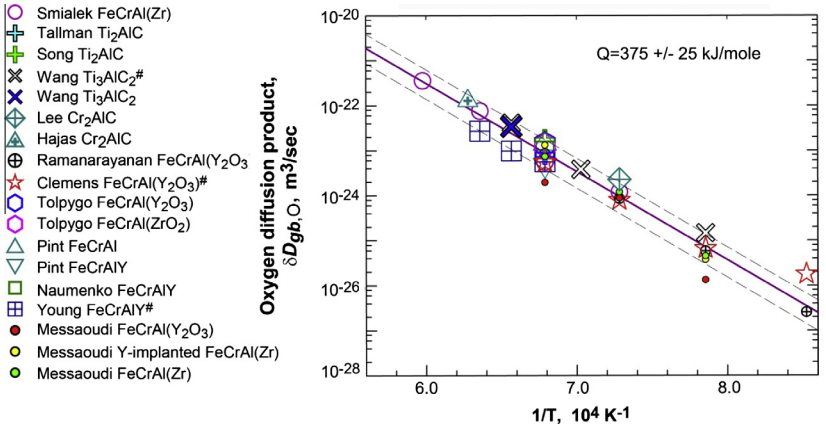

Fig. 2. Oxygen grain boundary diffusivity from MAX phases in Fig. 1 compared to other FeCrAl(X) alloy behavior. Calculated from oxidation data for undoped and Y, Zr, Y_2O_3, and ZrO_2 doped FeCrAl.

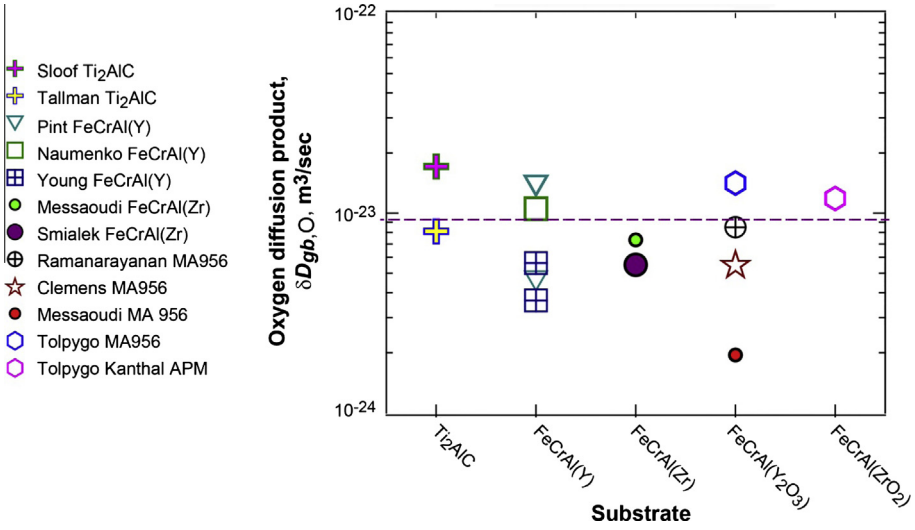

Fig. 3. Expanded 1200 °C diffusivity data from Fig. 2 showing overlap and range of variations for specific material classes.

Precise relations for scale thickness and interfacial grain size were reported for MA 956 and Kanthal APM (ZrO_2-oxide dispersed FeCrAl) oxidized at 1200 °C for up to 300 h [22]. In that study, the scale thickness (x) and grain size (G) were precisely characterized by microstructural analyses and described by the power law relations below. A and B are scale growth constants, while m and k are grain growth constants, as listed in Table 2:

$$x^2 = At + B\frac{G^m - G_0^m}{Gk(m-1)} \tag{13}$$

$$G = (G_0^m + kt)^{1/m} \tag{14}$$

It then follows from Eqs. 2a, 13 and 14 that:

$$\Pi = AG_i + B/m \tag{15}$$

Table 2
Tolpygo's FeCrAl(X) oxidation and scale grain enlargement constants for kinetic Eqs. 13–15 [22].

	A ((μm)²/h)	B	G_0 (μm)	k	m
MA956	0.046	2.55	0.176	0.015	4.47
APM	−0.023	1.85	0.362	0.016	3.47

The corresponding $\delta D_{gb,O,int.}$, given as hexagons in Figs. 2 and 3, are slightly above the FeCrAl(Zr) reference line, in juxtaposition to some of the previous values below the line. Overall, reasonable consistency is seen for $\delta D_{gb,O,int.}$ determined for the various FeCrAl(X) alloys and in the same range as the MAX phase alloys.

While a single value of Π is sufficient to warrant inclusion in the previous plots, a number of these studies followed kinetics and grain size over a substantial time interval. This allows the determination of multiple values of Π versus time at one temperature and leads to highly validated and robust average values of $\delta D_{gb,O,int.}$. Examples of the studies that provided detailed kinetic fits at 1200 °C, and thus Π versus t, are provided in Fig. 4 [7,10,19,22]. The FeCrAl(Zr) behavior had been presented for 1100°, 1200°, 1300° and 1400 °C in a more compressed plot [10]. Here appreciable drops in Π_i were noted at long 500–1000 h exposures. This suggests a reduction in δD_{gb} or an increase in $p_{O_2,int}$, perhaps due to changes in the dopant distribution through the scale thickness or aluminum depletion at the interface, respectively. (These and alternate attempts at explaining the decrease have not been verified and remain speculative). Much of the remaining data indicates periods of nearly constant values, as expected for scale growth controlled by a constant value of $\delta D_{gb,O,int.}$ at a given temperature. This is especially born out for the 2000 h FeCrAlY and 2800 h Ti_2AlC results [7,19].

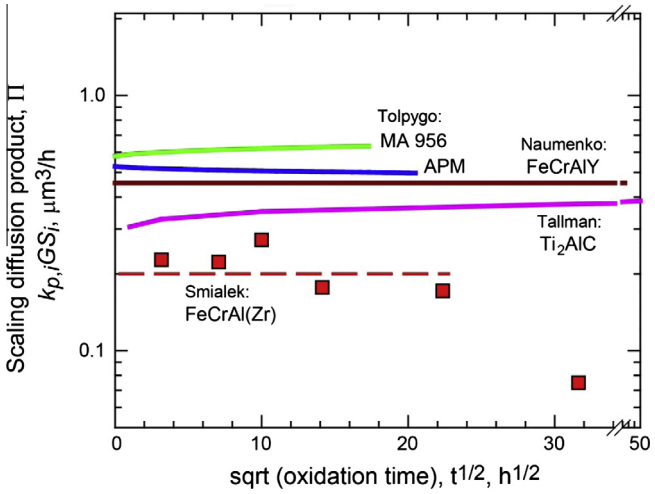

Fig. 4. Time invariant oxidation product, Π, at 1200 °C for Ti_2AlC MAX phase and four FeCrAl(X) alloys.

It is significant that the treatment presented above produced a nearly uniform assessment of data from 13 studies for 13 materials. There are no consistent or dramatic differences between substrates and scales presumably doped with Fe, Cr, Ti, Zr, or Y, with perhaps the largest reduction (3×) shown by Y-doping [13]. Given that all the validated data falls within tight bands shown in Fig. 2, it can be expected that variation limits for the activation energy may be so defined. It is found that these bands define a slope, with $Q \approx 375 \pm 25$ kJ/mol. This can be taken as a working value for the nearly invariant primary rate controlling factor for oxidation, i.e., inward oxygen grain boundary diffusion. It is subject to assumptions of minimal contributions from Al diffusion. Slight variability may also be expected from different oxidation environments, such as dry or humid Ar–O_2, N_2–O_2, or pure O_2, which are not differentiated or addressed here. It is nevertheless more fundamental than activation energies obtained from the oxidation constant alone, now widely accepted to be affected by an indeterminate, temperature dependent, interfacial grain expansion process. Alternatively, more attention can be focused on the oxidation product, Π, as proposed for FeCrAl(Zr) [10], to serve as a more invariant constant (and equivalent to '2C' in [19].

These values for $\delta D_{gb,O,int.}$ and activation energy enable more direct comparisons to diffusivity measured for bulk alumina. The oxidation analysis produced diffusivities an order of magnitude lower than those predicted from bulk alumina permeability studies for the pertinent $p_{O_2,int}$, with corresponding activation energies of 375 kJ/mol and 300 kJ/mol, respectively. These discrepancies were discussed at length without a completely satisfactory resolution [10]. Dopant effects and atomistic models of transport may account for some differences and provide deeper insight into mechanisms [23–27]. Some aluminum outward diffusion is well-documented, but is considered to be less important for thick established scales, since oxygen inward diffusion predominates through the majority of the scale [11]. These topics warrant further discussion and analysis. At present they cannot totally resolve the slight discrepancy with values predicted from bulk permeability studies and are considered beyond the scope of this paper.

It is recalled that the $\Pi/12$ solution was enabled by using the $p_{O_2}^{-1/6}$ dependence of oxygen diffusion obtained in [11] and Eq. (1). Its possible role, associated with creating doubly charged oxygen vacancies, $V_O^{\circ\circ}$, as predicted from classic Kroger–Vink equilibrium and charge neutrality conditions, has been raised previously, for example in [21,12,13,20]. The solution from [12] also highlighted the dominant $p_{O_2,int}$ aspect of controlling inward oxygen diffusion, in contrast to the external pressure, $p_{O_2,gas}$. Ultimately, this leads to simplified integration and a concise working relation, as derived in Eq. (3) [10]. By addressing the appropriate $p_{O_2,eq}$ corrections (from Eq. (6)), a more general relation along the format of Eq. (1) is obtained for these scales:

$$\delta D_{gb,O} = 7.567 \times 10^{-8} \exp\left(\frac{-Q}{RT}\right) p_{O_2}^{-1/6} \quad (16)$$

where Q is now found to be 544 kJ/mol. This is useful for comparisons to direct tracer studies in bulk alumina performed under atmospheric conditions. For the latter conditions, Eq. (16) indicates that bulk values are lower than those determined for alumina scale growth by a factor of 10^2–10^5 [10].

3. Conclusions

Published oxidation data for Ti_3AlC_2, Ti_2AlC, and Cr_2AlC MAX phase compounds have been analyzed by recent modifications of the Wagner integral that yield the relation for oxidation product $\Pi = 12\delta D_{gb,O,int.}$. The diffusivity values so determined were found to be in the same population as those extracted from numerous similar studies of FeCrAl(X) oxidation. While measureable scatter exists, neither group showed any large or consistent trend with Fe, Cr, Ti, Zr, Y, ZrO_2, or Y_2O_3 doping. Thus most behavior is adequately described by the general relation (in m^3/s), developed for FeCrAl(Zr), i.e., Eq. (4):

$$\delta D_{gb,O,int} = 1.8 \times 10^{-10} \exp\left(\frac{-Q}{RT}\right)$$

where Q was found to be 375 ± 25 kJ/mol. Oxidation results were shown for single values of Π as well as those obtained from multiple detailed measurements, sometimes spanning thousands of hours at a given temperature. Studies assuming a constant diffusion product with respect to p_{O_2}, (i.e., $\delta D^{\times}_{gb,O}$), were multiplied by the factor 1/6 $\Delta\ln[p_{O_2}]$. This produced values consistent with the present Wagner solution where $\delta D_{gb,O}$ was assumed to vary as $p_{O_2}^{-1/6}$. In summation, a large population of alumina scale kinetic data, normalized by grain size and spanning 900° to 1400 °C, cluster about a single relation based on oxygen grain boundary diffusion control.

Acknowledgements

The author is very grateful to V. Tolpygo, D. Naumenko, M. Barsoum, D. Tallman, and N. Jacobson for helpful discussions and sharing their results.

References

[1] M.W. Barsoum, T. El-Raghy, The MAX phases: unique new carbide and nitride materials, Am. Sci. 89 (2001) 334–343.
[2] X.H. Wang, Y.C. Zhou, High-temperature oxidation behavior of Ti_2AlC in air, Oxid. Met. 59 (2003) 303–320.
[3] X.H. Wang, Y.C. Zhou, Oxidation behavior of Ti_3AlC_2 at 1000–1400 °C in air, Corros. Sci. 45 (2003) 891–907.
[4] D.B. Lee, S.W. Park, Oxidation of Cr_2AlC between 900 and 1200 °C in air, Oxid. Met. 68 (2007) 211–222.
[5] J.L. Smialek, A. Garg, Microstructure and Oxidation of a MAX Phase/Superalloy Hybrid Interface, NASA/TM—2014-216679.
[6] X.H. Wang, F.Z. Li, J.X. Chen, Y.C. Zhou, Insights into high temperature oxidation of Al_2O_3-forming Ti_3AlC_2, Corros. Sci. 58 (2012) 95–103.
[7] D.J. Tallman, B. Anasori, M.W. Barsoum, A critical review of the oxidation of Ti_2AlC, Ti_3AlC_2 and Cr_2AlC in air, Mater. Res. Lett. 1 (2013) 115–125.
[8] G.M. Song, V. Schnabel, C. Kwakernaak, S. van der Zwaag, J.M. Schneider, W.G. Sloof, High temperature oxidation behaviour of Ti_2AlC ceramic at 1200°C, Mater. High Temp. 29 (2012) 205–209.
[9] D. Clemens, K. Bongartz, W.J. Quadakkers, H. Nickel, H. Holzbrecher, J.S. Becker, Determination of lattice and grain boundary diffusion coefficients in protective alumina scales on high temperature alloys using SEM, TEM and SIMS, Anal. Bioanal. Chem. 353 (1995) 267–270.

[10] J.L. Smialek, N.S. Jacobson, B. Gleeson, D. Hovis, A.H. Heuer, Oxygen Permeability and Grain-Boundary Diffusion Applied to Alumina Scales, NASA/TM—2013-217855.
[11] M. Wada, T. Matsudaira, S. Kitaoka, Mutual grain-boundary transport of aluminum and oxygen in polycrystalline Al_2O_3 under oxygen potential gradients at high temperatures, J. Ceram. Soc. Jpn. 119 (2011) 832–839.
[12] B.A. Pint, The Effect of Reactive Elements on the Growth of Al_2O_3 Scales, Ph.D. Dissertation, Massachusetts Institute of Technology, 1992.
[13] B.A. Pint, R.M. Deacon, Comment on: Oxidation of alloys containing aluminum and diffusion in Al_2O_3, J. Appl. Phys. 97 (2005) 116111-1–116111-3.
[14] D.J. Young, D. Naumenko, L. Niewolak, E. Wessel, L. Singheiser, W.J. Quadakkers, Oxidation kinetics of Y-doped FeCrAl-alloys in low and high pO_2 gases, Mater. Corros. 61 (2010) 838–844.
[15] C.W. Bale et al., FactSage thermochemical software and databases––recent developments, Calphad 33 (2009) 295–311.
[16] S.L. Chen et al., The PANDAT software package and its applications, Calphad 26 (2002) 175–188.
[17] D.B. Lee, T.D. Nguyen, S.W. Park, Long time oxidation of Cr_2AlC between 700 and 1000 °C in air, Oxid. Met. 77 (2002) 275–287.
[18] D.E. Hajas, M. to Baben, B. Hallstedt, R. Iskandar, J. Mayer, J.M. Schneider, Surf. Coat. Technol. 206 (2011) 591–598.
[19] D. Naumenko, B. Gleeson, E. Wessel, L. Singheiser, W.J. Quadakkers, Correlation between the microstructure, growth mechanism, and growth kinetics of alumina scales on a FeCrAlY alloy, Metall. Mater. Trans. A 38 (2007) 2974–2983.
[20] K. Messaoudi, A.M. Huntz, B. Lesage, Diffusion and growth mechanism of Al_2O_3 scales on ferritic Fe–Cr–Al alloys, Mater. Sci. Eng. A 247 (1998) 248–262.
[21] T.A. Ramanarayanan, M. Raghavan, R. Petkovic-Luton, The characteristics of alumina scales formed on Fe-based yttria-dispersed alloys, J. Electrochem. Soc. 131 (1984) 923–931.
[22] V. Tolpygo, Grain coarsening in alumina scales and its effect on the oxidation kinetics of Fe–Cr–Al alloys, presentation, in: P. Steinmetz, I.G. Wright (Chairs), 7th High Temperature Corrosion and Protection of Materials, European Federation of Corrosion, les Embiez, 2008.
[23] T. Matsudaira, M. Wada, S. Kitaoka, Effect of dopants on the distribution of aluminum and oxygen fluxes in polycrystalline alumina under oxygen potential gradients at high temperatures, J. Am. Ceram. Soc. 9 (2013) 1–9.
[24] T. Matsudaira, M. Wada, T. Saitoh, S. Kitaoka, The effect of lutetium dopant on oxygen permeability of alumina polycrystals under oxygen potential gradients at ultra-high temperatures, Acta Mater. 58 (2010) 1544–1553.
[25] T. Matsudaira, M. Wada, T. Saitoh, S. Kitaoka, Oxygen permeability in cation-doped polycrystalline alumina under oxygen potential gradients at high temperatures, Acta Mater. 59 (2011) 5440–5450.
[26] A.H. Heuer, D.B. Hovis, J.L. Smialek, B. Gleeson, Alumina scale formation: a new perspective, J. Am. Ceram. Soc. 94 (2011) 146–153.
[27] A.H. Heuer, T. Nakagawa, M.Z. Azar, D.B. Hovis, J.L. Smialek, B. Gleeson, M.W. Finnis, et al., On the growth of Al_2O_3 scales, Acta Mater. 61 (2013) 6670–6683.